



Implementation and Validation of Finite Volume C++ Codes for Plane Stress Analysis

Chakrit Suvanjumrat and Ekachai Chaichanasiri*

Department of Mechanical Engineering, Faculty of Engineering, Mahidol University, Nakornpathom, Thailand 73170

*Corresponding Author: teecc@mahidol.ac.th, Telephone 662 8892138 ext. 6409, Fax. 662 8892138 ext. 6429

Abstract

The interaction between solid and fluid is an important and interesting subject for the present. In general, to simulate the interaction between solid and fluid, finite element method (FEM) and finite volume method (FVM) are used for analysis of solid and fluid respectively. The transformation of results between FVM and FEM has a disadvantage since it takes time to transfer data between FEM and FVM. The individual using FVM for analysis of solid and fluid can avoid transferring data and it is more stable when simulating complicated problems. This research presented the FVM codes using C++ to perform a plane stress analysis. The code was implemented using Open Source Software that was OpenFOAM. The written code was validated with plane stress problems as the test cases, which comprised the tension of thin rectangular plate with and without a circular hole at the center. The results of FVM were compared with the analytical solutions. From the results, the average difference between the FVM results and analytical solutions was less than 1.68%. These results suggested the potential of using FVM for stress analysis and it will be used for analyzing solid-fluid interaction.

Keywords: Finite volume method, Finite element method, C++, Stress analysis, OpenFOAM

1. Introduction

The interaction between solid and fluid is an interesting subject for the present. For example, a sloshing of liquid in vehicles [1,2], an impact of the Tsunami wave on buildings [3]. In general, to simulate the interaction between solid and fluid, finite element method (FEM) and finite volume method (FVM) are used. The FEM is used for analysis of solid and the FVM is used for analysis of fluid. The transformation of results between FVM and FEM has a disadvantage

since it takes time to transfer data between FEM and FVM. The FVM is inherently good at treating complicated, coupled and non-linear differential equations, widely present in fluid flows. The individual using FVM for analysis of solid and fluid can avoid transferring data and it is more stable when simulating complicated problems. This research presented the FVM codes using C++ to perform a plane stress analysis. The code was implemented using Open Source Software that was OpenFOAM.

2. Materials and Methods

2.1 Governing Equation

The Cauchy's first law of motion for solid body was written in the differential equation,

$$\frac{\partial^2(\rho\bar{D})}{\partial t^2} = \nabla\sigma + \rho F_B \quad (1)$$

where \bar{D} was the displacement vector, σ was the stress tensor and F_B was the body force, respectively. The stress tensor in an isotropic linear elasticity was written as

$$\sigma = 2\mu\varepsilon + \lambda tr(\varepsilon)I \quad (2)$$

when
$$\varepsilon = \frac{1}{2}(\nabla\bar{D} + \nabla\bar{D}^T) \quad (3)$$

where I was the identity tensor, μ and λ were the Lamé's coefficients which could be written relating to the Young's modulus (E) and Poisson's ratio (ν) in plane stress,

$$\mu = \frac{E}{2(1+\nu)} \quad (4)$$

$$\lambda = \frac{E\nu}{(1+\nu)(1-\nu)} \quad (5)$$

Then Eq. (1) was arranged in the displacement vector form that

$$\frac{\partial^2(\rho\bar{D})}{\partial t^2} = \nabla\{\mu\nabla\bar{D} + \mu(\nabla\bar{D})^T + \lambda tr(\nabla\bar{D})I\} + \rho F_B \quad (6)$$

Equation (6) was completed to use for the governing equation of the solid body deformation. The initial condition consist of the specified distribution of \bar{D} and $\frac{\partial\bar{D}}{\partial t}$ at $t = 0$.

The boundary conditions could be of the fixed displacement, fixed traction, fixed pressure and plane of symmetry. The solution of Eq. (1) could be transformed using Eqs. (2) and (3) to determine strain and stress, respectively.

2.2 Finite Volume Discretization

The FVM consist of discretization of

the time interval and space. For the steady-state problems, the time step was effectively set to infinite. The space discretization subdivides the spatial domain into the number of polyhedral control volume (CV). Every internal face was shared by two CVs. A typical CV with a computational point p in its centroid was shown in Fig. 1. A sharing face was also marked and the neighboring CV had point nb in its centroid [4].

Equation (6) was expressed in the other form that

$$\frac{\partial^2(\rho\bar{D})}{\partial t^2} = \nabla\{(2\mu + \lambda)\nabla\bar{D}\} - \nabla\{\mu(\nabla\bar{D})^T + \lambda tr(\nabla\bar{D})I - (\mu + \lambda)\nabla\bar{D}\} + \rho F_B \quad (7)$$

For this research, considering μ and λ as constants thus

$$\nabla(\lambda tr(\nabla\bar{D})I) = \lambda\nabla(\nabla\bar{D}) \quad (8)$$

and
$$\nabla(\nabla\bar{D})^T = \nabla(\nabla\bar{D}) \quad (9)$$

Then Eq. (7) was rearranged that

$$\frac{\partial^2(\rho\bar{D})}{\partial t^2} = \nabla\{(2\mu + \lambda)\nabla\bar{D}\} + \rho F_B \quad (10)$$

The discretization of FVM uses the integral form of Eq. (10) over the CV around point p with the volume V . Using the Gauss theorem the following equation was

$$\frac{\partial}{\partial t} \int_V \frac{\partial(\rho\bar{D})}{\partial t} dV = \int_{S_f} (2\mu + \lambda)(\nabla\bar{D})\bar{n} dS_f + \int_V \rho F_B dV \quad (11)$$

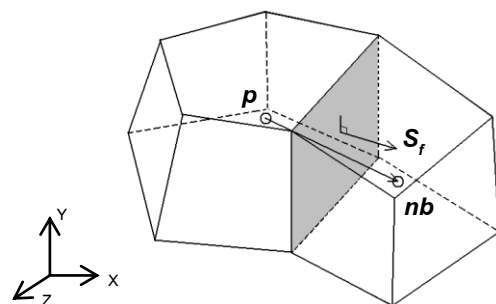


Fig. 1 Typical control volume system

The volume integral terms were evaluated using the mid-point rules [5]. The surface integral terms were split into the sum of integrals over the cell faces and also evaluated using the mid-point rules. The one equation assembled for each CV was

$$a_p \bar{D}_p = \sum a_{nb} \bar{D}_{nb} + S \quad (12)$$

when
$$a_p = (2\mu + \lambda) S_f \frac{\bar{D}_p}{d_{pn}^-}, \quad (13)$$

$$a_{nb} = (2\mu + \lambda) S_f \frac{\bar{D}_{nb}}{d_{pn}^-} \quad (14)$$

and
$$S = \rho V_p F_B \quad (15)$$

where d_{pn}^- was the distance between the mid-point p and the mid-point of neighbor CV (nb).

Thus creating a system of algebraic equations

$$[A][\bar{D}] = [S] \quad (16)$$

where $[A]$ was the sparse matrix with coefficients a_p on the diagonal and a_{nb} off the diagonal, $[\bar{D}]$ was the displacement vector for all CVs.

2.3 Validation of written C++ codes

The discretization method described in section 2.2 had been implemented in the Open Source Software, OpenFOAM, using C++ codes. The written code was validated with plane stress problems as the test cases, which comprised the tension of a thin rectangular plate with and without a circular hole at the center and the cross section of the plate was uniform. Figure 2 shows the geometry of the rectangular plate. According to Timoshenko and Goodier [6], an analytical solution for infinite width plate was justified for the finite width plate. When the width of the plate was not less than four times of the hole diameters, the error for $(\sigma_{\theta\theta})_{\max}$ was less than 6 percent. Based on Walter and Deborah [7], when the length of the plate was longer than

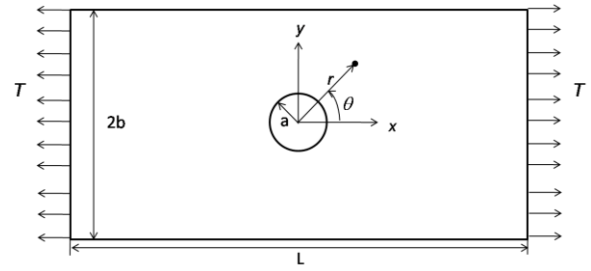


Fig. 2 Rectangular plate subjected to a uniform tension of magnitude T

its width, the plate could be considered as an infinite length and the effect from both end of the plate was negligible. Therefore, the width was 4 m, the length was 8 m and the thickness was 0.001 m. The hole situated at the center of the rectangular plate and had a diameter of 1 m.

All materials were assumed isotropic linear elastic. The Young's modulus was assumed 10000000 Pa and Poisson's ratio was assumed 0.3. Three cases of a rectangular plate subjected to a uniform tension of magnitude T in the x direction were analyzed. The first case was a rectangular plate without a hole. The second case was a rectangular plate with the hole. The third case was a quarter of a plate with the hole. This case was modeled based on symmetry of the plate. The magnitude of the tension used for all cases were 10000 Pa distributed uniformly along both sides of the rectangle as shown in Fig. 2. The plate was discretized as shown in Fig. 3. The results of FVM were compared with the analytical solutions for all cases.

3. Results and Discussion

3.1 Rectangular plate without the hole

In this load case, the plate was subjected to a uniform tension of 10000 Pa. Therefore, this was an analytical solution of σ_{xx} for this case. The distribution of σ_{xx} , σ_{yy} and σ_{xy} calculated by FVM was shown in Fig. 4.

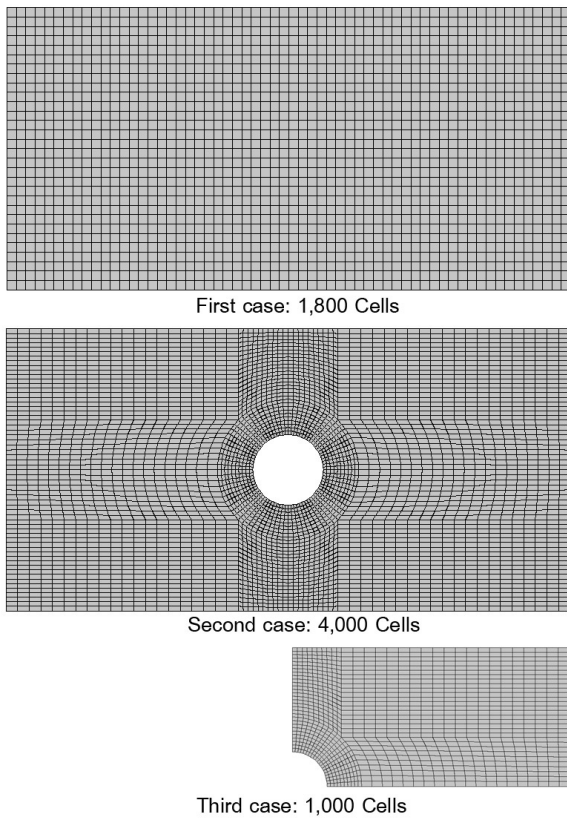


Fig. 3 Discretized plates for FVM

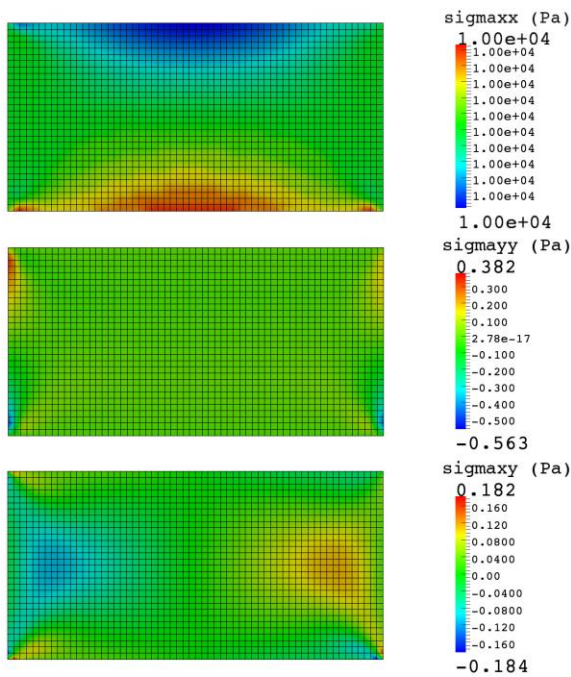


Fig. 4 The distribution of σ_{xx} , σ_{yy} and σ_{xy} for the first case calculated by FVM

It could be seen that the stress distributions were slightly difference between the

center and the edges of the plate. The average values of σ_{xx} , σ_{yy} and σ_{xy} from every center point of cells were 9999.997, 0.000291 and 0.00116 Pa, respectively. These were due to approximation error, which was the nature of numerical methods. When compared with the analytical result, it was found that the average difference of σ_{xx} from every point between the FVM and analytical solution was only -0.00003 %.

3.2 Rectangular plate with the hole

The analytical solution for this case was based on a plate with infinite width [6].

$$\sigma_{rr} = \frac{T}{2} \left(1 - \frac{a^2}{r^2} \right) + \frac{T}{2} \left(1 + \frac{3a^4}{r^4} - \frac{4a^2}{r^2} \right) \cos 2\theta \quad (17)$$

$$\sigma_{\theta\theta} = \frac{T}{2} \left(1 + \frac{a^2}{r^2} \right) - \frac{T}{2} \left(1 + \frac{3a^4}{r^4} \right) \cos 2\theta \quad (18)$$

$$\sigma_{r\theta} = -\frac{T}{2} \left(1 - \frac{3a^4}{r^4} + \frac{2a^2}{r^2} \right) \sin 2\theta \quad (19)$$

, where a was a radius of a circle, r was a radius from center of the plate to any points on the plate and θ was the angle between the x -axis of the plate to the radius (Fig. 2). The σ_{rr} , $\sigma_{\theta\theta}$ and $\sigma_{r\theta}$ could be transformed to x - y coordinates by the relation [6]

$$\sigma_{xx} = \sigma_{rr} \cos^2 \theta + \sigma_{\theta\theta} \sin^2 \theta - 2\sigma_{r\theta} \sin \theta \cos \theta \quad (20)$$

$$\sigma_{yy} = \sigma_{rr} \sin^2 \theta + \sigma_{\theta\theta} \cos^2 \theta + 2\sigma_{r\theta} \sin \theta \cos \theta \quad (21)$$

$$\sigma_{xy} = (\sigma_{rr} - \sigma_{\theta\theta}) \sin \theta \cos \theta + \sigma_{r\theta} (\cos^2 \theta - \sin^2 \theta) \quad (22)$$

Therefore the analytical solution in terms of σ_{xx} , σ_{yy} and σ_{xy} was [8]

$$\sigma_{xx} = T \left(1 - \frac{a^2}{r^2} \left(\frac{3}{2} \cos 2\theta + \cos 4\theta \right) + \frac{3a^4}{2r^4} \cos 4\theta \right) \quad (23)$$

$$\sigma_{yy} = T \left(-\frac{a^2}{r^2} \left(\frac{1}{2} \cos 2\theta - \cos 4\theta \right) - \frac{3a^4}{2r^4} \cos 4\theta \right) \quad (24)$$

$$\sigma_{xy} = T \left(-\frac{a^2}{r^2} \left(\frac{1}{2} \sin 2\theta + \sin 4\theta \right) + \frac{3a^4}{2r^4} \sin 4\theta \right) \quad (25)$$

where $r = \sqrt{x^2 + y^2}$ and $\theta = \tan^{-1} \frac{y}{x}$.

Figure 5 shows the distribution of σ_{xx} , σ_{yy} and σ_{xy} calculated by FVM. As

expected, the local high stress was observed around the hole. The σ_{xx} , σ_{yy} and σ_{xy} were compared with analytical solution using 16 points as shown in Fig. 6. These points were selected based on radial and angle position around the hole at $r = 0.5, 1, 1.5, 2$ m and $\theta = 0^\circ, 30^\circ, 60^\circ, 90^\circ$. The order of points was arranged by starting from $r = 0.5$ m to $r = 2$ m and $\theta = 0^\circ$ to 90° . The first point was the position $r = 0.5$ m and $\theta = 0^\circ$.

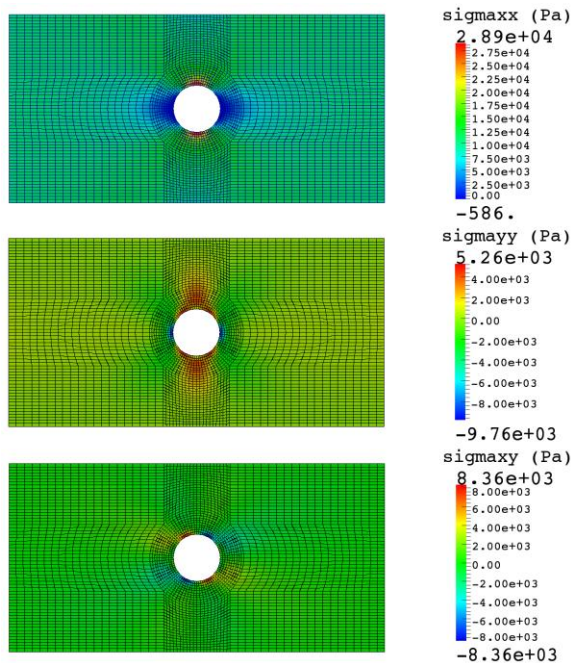


Fig. 5 The distribution of σ_{xx} , σ_{yy} and σ_{xy} for the second case calculated by FVM

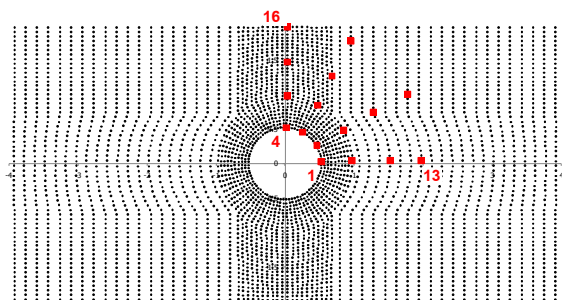


Fig. 6 Points for stress comparison for the second case

The comparison of the σ_{xx} , σ_{yy} and σ_{xy} were shown in Tables. 1, 2 and 3, respectively. It could be seen that the difference of stresses of points at the boundary of the hole were higher than the other points. This effect was received from the curvature of the cells at the boundary.

Table. 1 Comparison of σ_{xx} between FVM and analytical solution for the second case

Point number	FVM σ_{xx} (Pa)	Analytical σ_{xx} (Pa)	Difference from analytical σ_{xx} (%)
1	-416.30	-330.63	25.91
2	3413.27	3597.09	-5.11
3	16005.10	15624.20	2.44
4	29259.20	26838.23	9.02
5	4442.75	4487.64	-1.00
6	8934.50	8659.02	3.18
7	13613.00	12787.65	6.45
8	13101.30	12365.01	5.95
9	7638.19	7490.16	1.98
10	10055.60	9612.16	4.61
11	11879.80	11380.62	4.39
12	11074.50	10775.73	2.77
13	8677.30	8460.72	2.56
14	10184.90	9780.92	4.13
15	11264.90	10729.02	4.99
16	9238.54	10382.83	-11.02
Average			3.83

Table. 2 Comparison of σ_{yy} between FVM and analytical solution for the second case

Point number	FVM σ_{yy} (Pa)	Analytical σ_{yy} (Pa)	Difference from analytical σ_{yy} (%)
1	-9884.64	-7781.94	27.02
2	-1264.15	-877.65	44.04
3	4580.28	3868.89	18.39
4	1210.02	1274.34	-5.05
5	109.29	366.56	-70.19
6	-2014.49	-1411.44	42.73
7	331.65	693.42	-52.17
8	2676.58	2886.57	-7.27
9	447.73	360.42	24.22
10	-851.95	-755.26	12.80
11	-665.92	-340.68	95.47
12	806.39	1520.56	-46.97
13	472.48	288.95	63.51
14	-208.17	-407.35	-48.90
15	-107.27	-204.51	-47.55
16	63.00	988.55	-93.63
Average			-2.72

Table. 3 Comparison of σ_{xy} between FVM and analytical solution for the second case

Point number	FVM σ_{xy} (Pa)	Analytical σ_{xy} (Pa)	Difference from analytical σ_{xy} (%)
1	-83.41	-136.01	-38.67
2	-2011.28	-2311.09	-12.97
3	-7640.67	-6808.15	12.23
4	-1021.22	-871.72	17.15
5	-374.93	-352.57	6.34
6	-2684.99	-2542.52	5.60
7	931.07	634.31	52.75
8	195.04	145.92	33.66
9	-126.77	-118.36	7.10
10	-1236.09	-1312.84	-5.85
11	839.49	507.70	65.35
12	98.50	67.19	46.60
13	-62.50	-56.88	9.88
14	-764.98	-743.48	2.89
15	312.76	257.37	21.52
16	20.01	32.38	-38.18
Average			11.59

3.3 A quarter of the rectangular plate with the hole

For this case, the distribution of σ_{xx} , σ_{yy} and σ_{xy} calculated by FVM was shown in Fig. 7. The localized high stress could be observed around the hole. The stress distribution pattern for this case was similar to Fig. 5. Figure 8 shows the location of points for stress comparison calculated by FVM and analytical solution. The analytical solution was calculated by the same equation as for the second case. From Tables. 4, 5 and 6, it could be seen that the difference of stresses were high at the boundary of the hole as same as the second case.

4. Conclusion

In this research, the FVM that was developed for computational fluid dynamics was applied to analyze solid mechanics. The plane stress problems were used as a test case. The code for the FVM was written using C++ language and implemented in the Open Source Software, OpenFOAM. The obtained results were corresponded to the analytical solution. For the

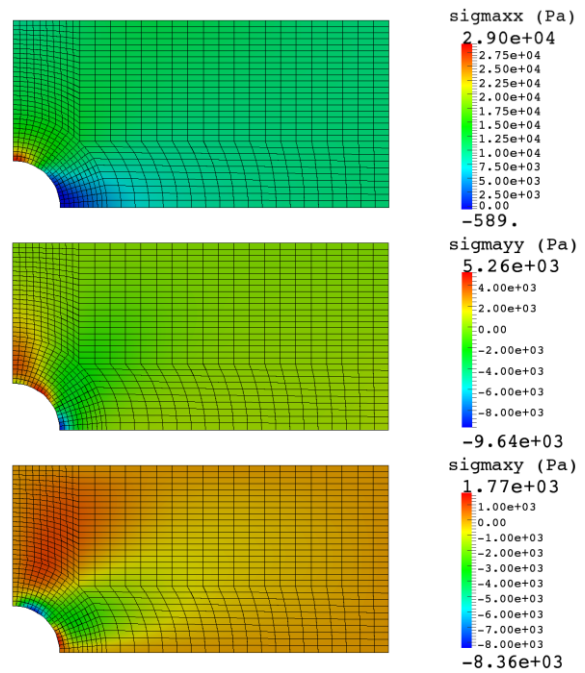


Fig. 7 The distribution of σ_{xx} , σ_{yy} and σ_{xy} for the third case calculated by FVM

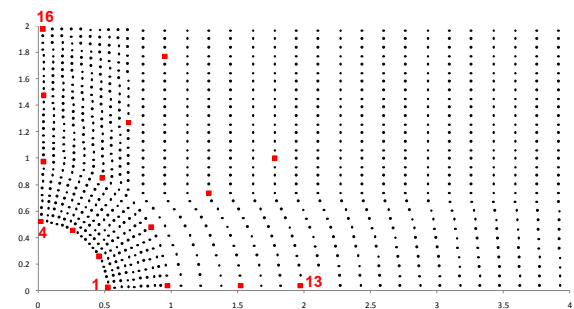


Fig. 8 Points for stress comparison for the third case

Table. 4 Comparison of σ_{xx} between FVM and analytical solution for the third case

Point number	FVM σ_{xx} (Pa)	Analytical σ_{xx} (Pa)	Difference from analytical σ_{xx} (%)
1	-388.85	-330.63	17.61
2	3413.45	3597.09	-5.11
3	16008.00	15624.20	2.46
4	29242.00	26838.23	8.96
5	4467.10	4487.64	-0.46
6	8933.62	8659.02	3.17
7	13613.20	12787.65	6.46
8	13064.00	12365.01	5.65
9	7653.89	7490.16	2.19
10	10054.90	9612.16	4.61
11	11879.60	11380.62	4.38
12	11066.90	10775.73	2.70
13	8684.08	8460.72	2.64
14	10184.50	9780.92	4.13
15	11264.40	10729.02	4.99
16	9275.68	10382.83	-10.66
Average			3.36



Table. 5 Comparison of σ_{yy} between FVM and analytical solution for the third case

Point number	FVM σ_{yy} (Pa)	Analytical σ_{yy} (Pa)	Difference from analytical σ_{yy} (%)
1	-9704.68	-7781.94	24.71
2	-1270.84	-877.65	44.80
3	4581.00	3868.89	18.41
4	1209.50	1274.34	-5.09
5	139.71	366.56	-61.89
6	-2014.19	-1411.44	42.70
7	331.60	693.42	-52.18
8	2663.81	2886.57	-7.72
9	454.11	360.42	25.99
10	-851.15	-755.26	12.70
11	-665.59	-340.68	95.37
12	798.44	1520.56	-47.49
13	474.94	288.95	64.37
14	-207.72	-407.35	-49.01
15	-107.26	-204.51	-47.55
16	65.77	988.55	-93.35
Average			-2.20

Table. 6 Comparison of σ_{xy} between FVM and analytical solution for the third case

Point number	FVM σ_{xy} (Pa)	Analytical σ_{xy} (Pa)	Difference from analytical σ_{xy} (%)
1	-212.79	-416.48	-48.91
2	-2012.40	-2311.09	-12.92
3	-7641.70	-6808.15	12.24
4	-1041.32	-871.72	19.46
5	-232.35	-352.57	-34.10
6	-2686.51	-2542.52	5.66
7	969.32	634.31	52.81
8	87.58	145.92	-39.98
9	-82.11	-118.36	-30.63
10	-1236.45	-1312.84	-5.82
11	824.49	496.06	66.21
12	50.08	67.19	-25.46
13	-41.00	-56.88	-27.92
14	-764.77	-743.48	2.86
15	312.72	257.37	21.51
16	87.07	103.47	-15.85
Average			-3.80

plate without the hole, the results were slightly difference from the analytical solution. For the plate with a hole, the FVM could capture the localized stress concentration. The quarter of a plate with a hole had the results similar to the full plate. Therefore, the symmetry model was justified. The overall difference of the stress calculated by FVM from analytical solution was less than 1.68 %. These results suggested the

potential of using FVM for stress analysis and it will be used for analyzing solid-fluid interaction.

5. References

[1] Romero, J.A., Ramirez, O., Fortanell, J.M., Martinez, M. and Lozano, A. (2006). Analysis of lateral sloshing forces within road containers with high fill levels, *Proceedings of the Institution of Mechanical Engineers, Part D: Journal of Automobile Engineering*, vol.220(3), pp. 302-312.

[2] Kim, H.S. and Lee, Y.S. (2008). Optimization design technique for reduction of sloshing by evolutionary methods, *Journal of Mechanical Science and Technology*, vol.22(1), pp. 25-33.

[3] Thusyanthan, N.I. and Madabhushi, S.P.G. (2008). Tsunami wave loading on coastal houses: A model approach, *Proceedings of the Institution of Civil Engineers: Civil Engineering*, vol.161(2), pp. 77-86.

[4] OpenFOAM. (2009). *User Guide Version 1.6*, edition, OpenCFD Limited, London.

[5] Jasak, H. and Weller, H.G. (2000). Application of the finite volume method and unstructured meshes to linear elasticity, *International Journal for Numerical Methods in Engineering*, vol.48(2), pp. 267-287.

[6] Timoshenko, S.P. and Goodier, J.N. (1982). *Theory of Elasticity*, 3rd edition, McGraw-Hill, London.

[7] Walter, D.P. and Deborah, F.P. (2008). *Peterson's Stress Concentration Factors*, 3rd edition, John Wiley & Sons, Inc., New Jersey.

[8] Demirdzic, I. and Muzaferija, S. (1994). Finite volume method for stress analysis in complex domains, *International Journal for Numerical Methods in Engineering*, vol.37(21), pp. 3751-3766.